

Supporting Information

Site-Selective Synthesis and Concurrent Immobilization of Imine-Based Covalent Organic Frameworks on Electrodes Using an Electrogenerated Acid

*T. Shirokura, T. Hirohata, K. Sato, E. Villani, K. Sekiya, Y.-A. Chien, T. Kurioka, R. Hifumi, Y. Hattori, M. Sone, I. Tomita, S. Inagi**

Contents

1. Materials	3
2. General	4
3. Synthesis	6
3-1. Synthesis of TAPB-PDA COF	6
3-2. Synthesis of TAPB-OMePDA COF	6
3-3. Synthesis of TAPT-PDA COF	6
3-4. Synthesis of TAPT-OMePDA COF	6
3-5. Synthesis of TAPM-PDA COF	6
4. DPH as an electrogenerated acid (EGA) source	7
5. TAPB-PDA COF synthesis under various conditions	8
6. Characterization and properties of TAPB-PDA COF	12
7. Characterization and properties of a series of electrosynthesized COF	14
8. Reference	20

1. Materials

Acetonitrile (MeCN) (spectrophotometry grade), chloroform (spectrophotometry grade), dichloromethane (DCM) (spectrophotometry grade), *N,N*-dimethylformamide (DMF) (spectrophotometry grade), dimethyl sulfoxide (DMSO), mesitylene, nitromethane (MeNO₂), tetrahydrofuran (THF) (spectrophotometry grade) and toluene were purchased from FUJIFILM Wako Pure Chemical Corporation. Chloroform-*d*₁ (CDCl₃), 99.8% with 0.03 vol% tetramethylsilane (TMS), 1,4-dioxane, ethanol (EtOH), ethyl acetate (EtOAc), *n*-hexane were purchased from Kanto Chemical Co., Inc. Methyl yellow, tetrabutylammonium hexafluorophosphate (Bu₄NPF₆), tetrakis(4-aminophenyl)methane (TAPM), 4,4',4''-(1,3,5-triazine-2,4,6-triyl)trianiline (TAPT), 1,3,5-tris(4-aminophenyl)benzene (TAPB) were purchased from TCI (Tokyo Chemical Industry Co., Ltd.). 2,5-Dimethoxybenzene-1,4-dicarboxaldehyde (OMePDA), 1,2-diphenylhydrazine (DPH) and terephthalaldehyde (PDA) were purchased from Sigma-Aldrich. Acetone and methanol (MeOH) were purchased from Godo. Potassium bromide (KBr) was purchased from NACALAI TESQUE, INC. Carbon dioxide (CO₂) used for supercritical CO₂ drying was purchased from Nippon Tansan Gas Co., Ltd., and had a purity of 99.99%. All reagents and solvents were used without purification unless otherwise noted. Bu₄NPF₆ was recrystallized from methanol, and dried before use.

2. General

Cyclic voltammetry (CV) measurements

Cyclic voltammetry was performed using an ALS instrument Bi-Potentiostat Model:2325. All voltammetry measurements were carried out in a three-electrode system equipped with an ITO (Indium Tin Oxide)-coated glass substrates (10 mm × 10 mm × 1.1 t (10 Ω/sq)) working electrode, a Pt plate counter electrode (20 mm × 20 mm) and an Ag/Ag⁺ reference electrode.

Constant potential electrolysis

Constant potential electrolysis was performed using a Hokuto denko HABF-501A potentiostat in a three-electrode system equipped with an ITO-coated glass substrate (10 mm × 10 mm × 1.1 t (10 Ω/ sq)) working electrode, a Pt plate counter electrode (20 mm × 20 mm) and an Ag/Ag⁺ reference electrode.

Fourier transform infrared spectroscopy (FT-IR) measurements

All FT-IR spectra were obtained on a Shimadzu IR Tracer-100 spectrophotometer. The samples were pellet-molded with KBr.

¹³C cross-polarization/magic angle spinning NMR (CP-MAS ¹³C NMR)

All CP-MAS ¹³C NMR spectra were recorded on a JEOL JNM-ECA400 spectrometer (100.7 MHz for ¹³C) using a 3.2 mm ϕ MAS probe.

X-ray photoelectron spectroscopy (XPS)

All XPS spectra were obtained on a ULVAC-PHI, VersaProbe III. The COF film samples on the ITO substrate were directly inserted to the measurement chamber.

Supercritical CO₂ drying

Supercritical CO₂ drying was conducted with designed high-pressure apparatus (Japan Spectra Company, Japan). The reactor used in the supercritical CO₂ drying was made of stainless steel 316 with polyether ether ketone (PEEK) coating on the inner wall, and its inner volume was 50 mL. Details of the apparatus can be found in a previous report.¹ Samples stored in hexane were placed in tea bags and set in the reactor while wet. After supercritical CO₂ drying was performed at 50°C and 9 MPa for 10 minutes, the pressure was returned to 1 atm. This operation was performed 20 times and the dried powder was collected.

Small-angle X ray scattering (SAXS) measurements

All SAXS diffraction patterns were collected with a Rigaku NANO-Viewer, X-ray diffractometer (CuK α radiation, $\lambda = 0.15405$ nm, 40 kV, and 30 mA). The powdered samples packed in glass tube were used for the measurement.

N₂ gas adsorption/desorption measurement (BET)

All surface area measurements were performed on a QUANTACHROME AUTOSORB MP/VP. Samples between 15 and 30 mg were packed in glass tubes. Specific surface area was calculated based on the Brunauer-Emmett-Teller (BET) model from the region of the pressure range P/P_0 of 0.05–0.35, and pore distribution was calculated using the density functional theory (DFT) model of cylinder-shaped carbon in the device based on the nonlocal density functional theory (NLDFE) method.

Thermogravimetric analysis (TGA) measurements

TGA analysis was performed on a Shimadzu TGA-50 analyzer. The samples were heated from room temperature to 800°C (10°C/min.) and held 15 min. under nitrogen flow (50 mL/min.).

NMR analysis

All NMR spectra were recorded on a Bruker model AVANCE III 400 spectrometer (400.13 MHz for ¹H) using CDCl₃ as a solvent at room temperature. The chemical shifts for ¹H NMR spectrum were given in δ (ppm) relative to internal TMS.

Scanning electron microscopy (SEM)

SEM images were taken with a JEOL JSM-6610 (accelerating voltage of 5 kV) microscope. The sample to be observed was Au-coated on the surface by an Eiko Co., Ltd. IB-3 ion coater.

Contact angle measurements

Contact angle measurements were carried out using a NiCK Co., Ltd. LSE-ME1 contact angle meter. Measurements were made immediately after a drop of purified water or *n*-hexadecane was added onto a COF film on an electrode.

3. Synthesis

3-1. Synthesis of TAPB-PDA COF

The electrolyte was prepared by dissolving 1,3,5-tris(4-aminophenyl)benzene (TAPB) (10 mM) and terephthalaldehyde (PDA) (15 mM) as monomers, 1,2-diphenylhydrazine (DPH) (20 mM) as an electrogenerated acid (EGA) source, and Bu_4NPF_6 (100 mM) as a supporting electrolyte in MeNO_2 . The electrolyte was transferred to a cell equipped with an ITO-coated glass electrode (10 mm \times 10 mm) as a working electrode, a Pt plate (20 mm \times 20 mm) as a counter electrode, and an Ag/Ag^+ reference electrode. After bubbling with Ar, electrolysis was performed by a potential sweep method at room temperature (potential range: -0.5 to 0.5 V at a scan rate of 20 mV/s for 20 cycles). The TAPB-PDA COF was obtained on the ITO electrode after rinsed with MeCN, MeOH, hexane, followed by supercritical CO_2 drying.

3-2. Synthesis of TAPB-OMePDA COF

The TAPB-OMePDA COF was prepared with the above procedure using TAPB (10 mM) and 2,5-dimethoxybenzene-1,4-dicarboxaldehyde (OMePDA) (15 mM) as monomers.

3-3. Synthesis of TAPT-PDA COF

The TAPT-PDA COF was prepared with the above procedure using 4,4',4''-(1,3,5-triazine-2,4,6-triyl)trianiline (TAPT) (10 mM) and PDA (15 mM) as monomers.

3-4. Synthesis of TAPT-OMePDA COF

The TAPT-OMePDA COF was prepared with the above procedure using TAPT (10 mM) and OMePDA (15 mM) as monomers.

3-5. Synthesis of TAPM-PDA COF

The TAPM-PDA COF was prepared with the above procedure using tetrakis(4-aminophenyl)methane (TAPM) (10 mM) and PDA (17 mM) as monomers in DMF. Due to a solubility issue, TAPM was dissolved in DMF first, and then the other substrates were added. The potential sweep electrolysis was performed for 10 cycles.

4. DPH as an electrogenerated acid (EGA) source

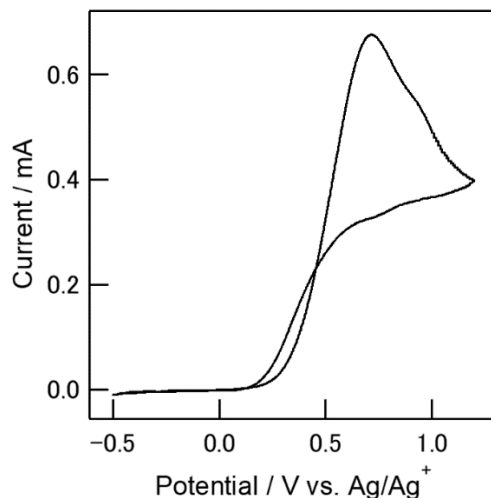


Figure S1. Cyclic voltammogram of DPH (5 mM) in 0.1 M Bu₄NPF₆/MeNO₂ using an ITO working electrode (10 mm × 10 mm), a Pt counter electrode (20 mm × 20 mm) and an Ag/Ag⁺ reference electrode at a scan rate of 20 mV s⁻¹.

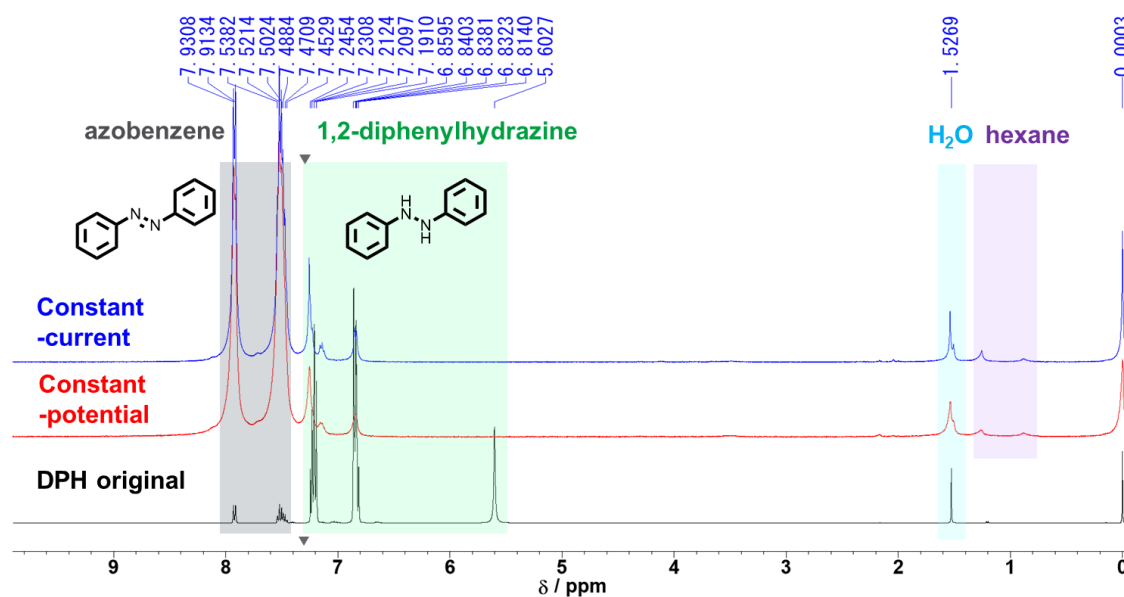


Figure S2. ¹H NMR spectra (CDCl₃) of (Black) DPH original, and DPH after electrolysis in 0.1 M Bu₄NPF₆/MeNO₂ using an ITO working electrode (10 mm × 10 mm), a Pt counter electrode (20 mm × 20 mm) and an Ag/Ag⁺ reference electrode: (Red) constant-potential electrolysis at 0.5 V vs. Ag/Ag⁺ and (Blue) constant-current electrolysis for 1.7 F/mol. The reaction mixture was purified by silica gel column chromatography (eluent; ethyl acetate: hexane = 1:1)

5. TAPB-PDA COF synthesis under various conditions

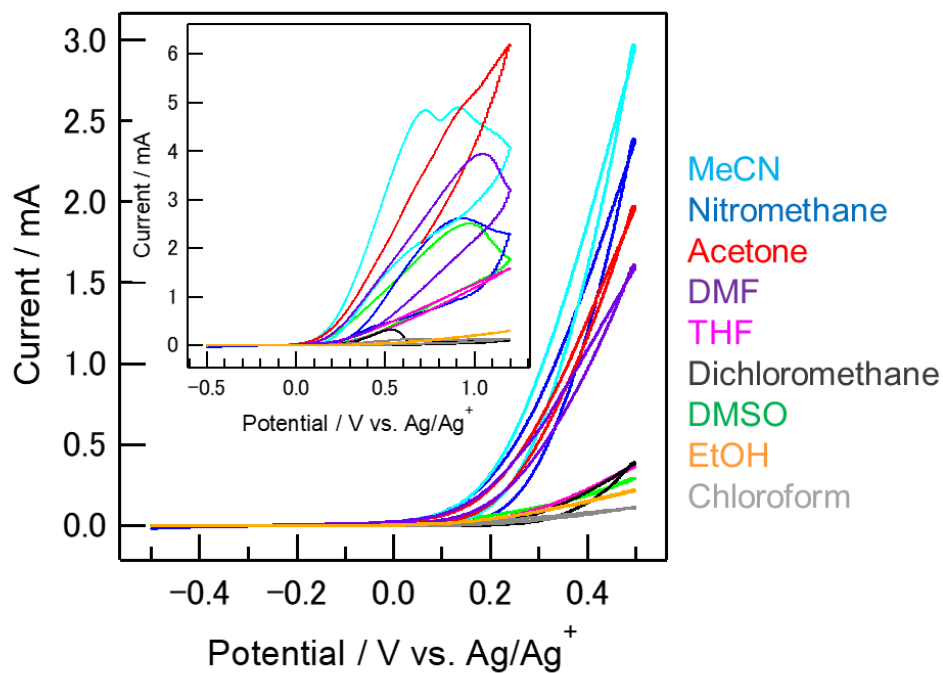


Figure S3. Cyclic voltammograms of TAPB (10 mM) + PDA (15 mM) + DPH (20 mM) in 0.1 M Bu_4NPF_6 /different solvents using an ITO working electrode (10 mm \times 10 mm), a Pt counter electrode (20 mm \times 20 mm) and an Ag/Ag^+ reference electrode at a scan rate of 100 mV s^{-1} .

Table S1. Photographs of the cells and ITO working electrodes after electrolysis of TAPB (10 mM) + PDA (15 mM) + DPH (20 mM) in various solvents. The electrolysis was performed by constant potential (0.2 or 0.4 V vs. Ag/Ag⁺) method in 0.1 M Bu₄NPF₆/solvent using an ITO working electrode (10 mm × 10 mm), a Pt counter electrode (20 mm × 20 mm) and an Ag/Ag⁺ reference electrode.

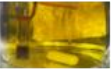


























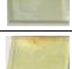




Entry	Solvent	Potential [V]	Time [min.]	Cell/ electrode image	
1	MeCN	0.2	30		
2		0.4	60		
3	Nitromethane	0.2	2		
4		0.4	5		
5	Acetone	0.2	60		
6		0.4	-	-	-
7	DMF	0.2	60		
8		0.4	-	-	-
9	THF	0.2	20		
10		0.4	30		
11	Dichloromethane	0.2	30		
12		0.4	15		
13	DMSO	0.2	3		
14		0.4	-		
15	EtOH	0.2	10		
16		0.4	10		
17	Chloroform	0.2	10		
18		0.4	10		

Table S2. Investigation of the conditions for TAPB-PDA COF electrosynthesis. The electrolysis was performed by a constant potential method in 0.1 M Bu₄NPF₆/MeNO₂ using an ITO working electrode (10 mm × 10 mm), a Pt counter electrode (20 mm × 20 mm) and an Ag/Ag⁺ reference electrode.





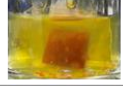





















Entry	Potential [V]	Concentration [mM]				Time [min.]	Charge [mC]	Cell/ electrode image	
		TAPB	PDA	DPH	Bu ₄ NPF ₆				
1	0.2	10	15	20	100	5	4.4		
2	0.3	10	15	20	100	5	9.3		
3	0.4	10	15	20	100	5	25.0		
4	0.5	10	15	20	100	5	50.7		
5	0.3	2.5	3.75	20	100	5	18.2		
6	0.5	2.5	3.75	20	100	5	103.6		
7	0.3	10	15	5	100	5	6.8		
8	0.5	10	15	5	100	5	27.8		
9	0.3	2.5	3.75	5	100	5	13.0		
10	0.5	2.5	3.75	5	100	5	90.1		

Table S3. Investigation of the conditions for TAPB-PDA COF electrosynthesis with the optimized substrate concentrations (TAPB (10 mM) + PDA (15 mM) + DPH (20 mM)). The electrolysis was performed by the potential-sweep method in 0.1 M $\text{Bu}_4\text{NPF}_6/\text{MeNO}_2$ using an ITO working electrode (10 mm \times 10 mm), a Pt counter electrode (20 mm \times 20 mm) and an Ag/Ag^+ reference electrode.

Entry	Potential range [V]	Cycle number [-]	Scan rate [mV/sec.]	Cell / electrode image
1	-0.5 – 0.2	20	20	
2	-0.5 – 0.3	20	20	
3	-0.5 – 0.4	20	20	
4	-0.5 – 0.5	20	20	
5	-0.5 – 0.5	20	50	
6	-0.5 – 0.5	20	100	

6. Characterization and properties of TAPB-PDA COF

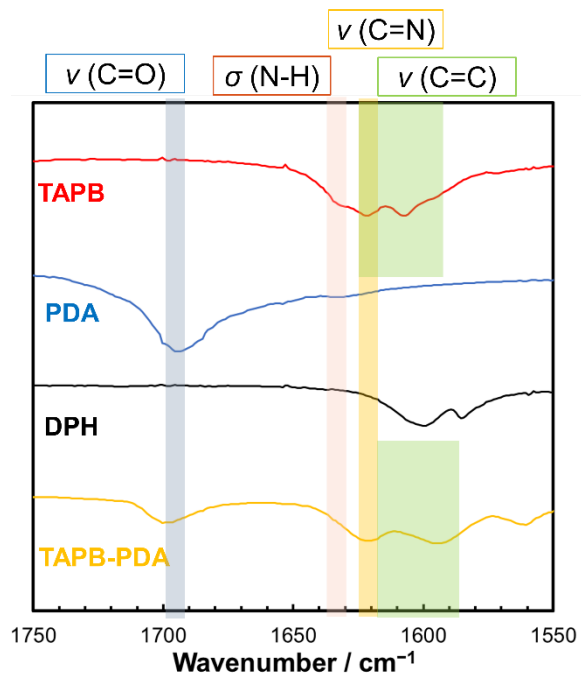


Figure S4. Enlarged detail of FT-IR spectra corresponding to Figure 4a.

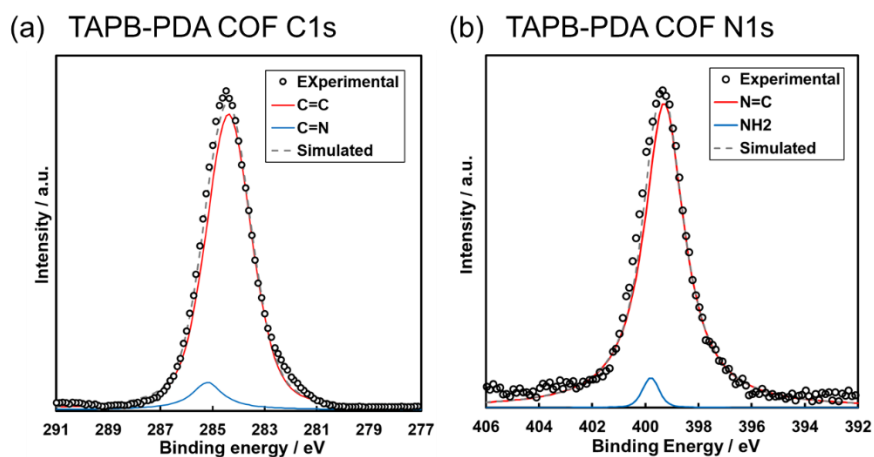


Figure S5. XPS spectra of the TAPB-PDA COF sample. (a) C1s, (b) N1s peak.

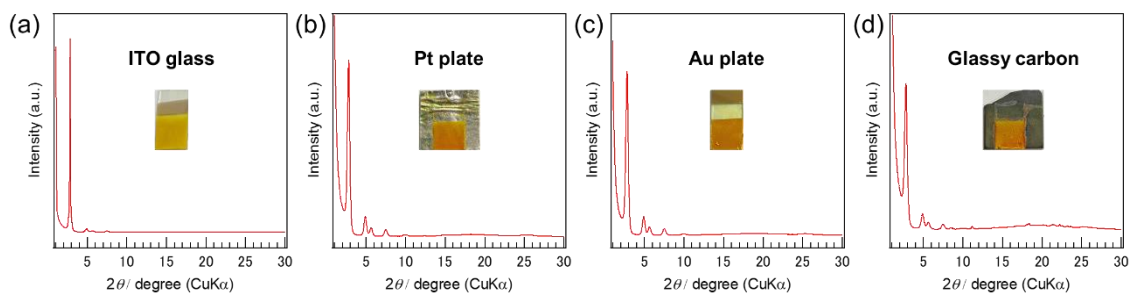


Figure S6. SAXS diffraction patterns of the TAPB-PDA COF onto different electrodes and the corresponding photographs of the electrodes. The samples were rinsed with MeCN, MeOH and hexane, and activated by supercritical CO_2 drying.

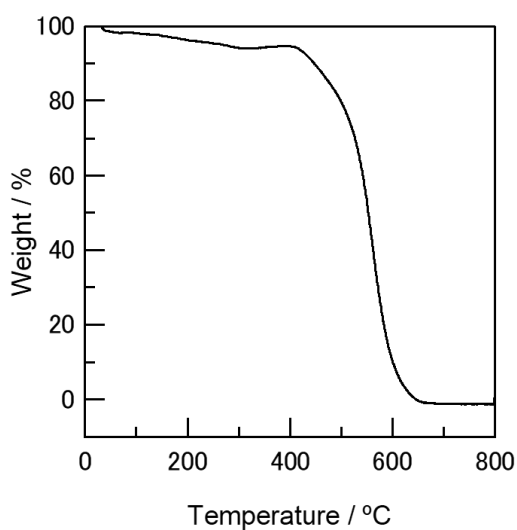


Figure S7. A thermogravimetric analysis (TGA) curve of the TAPB-PDA COF.

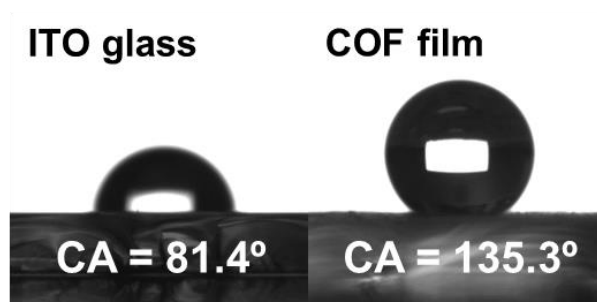


Figure S8. Contact angle measurements of a water droplet onto the ITO electrode (left) and onto the TAPB-PDA COF film (right).

7. Characterization and properties of a series of electrosynthesized COF

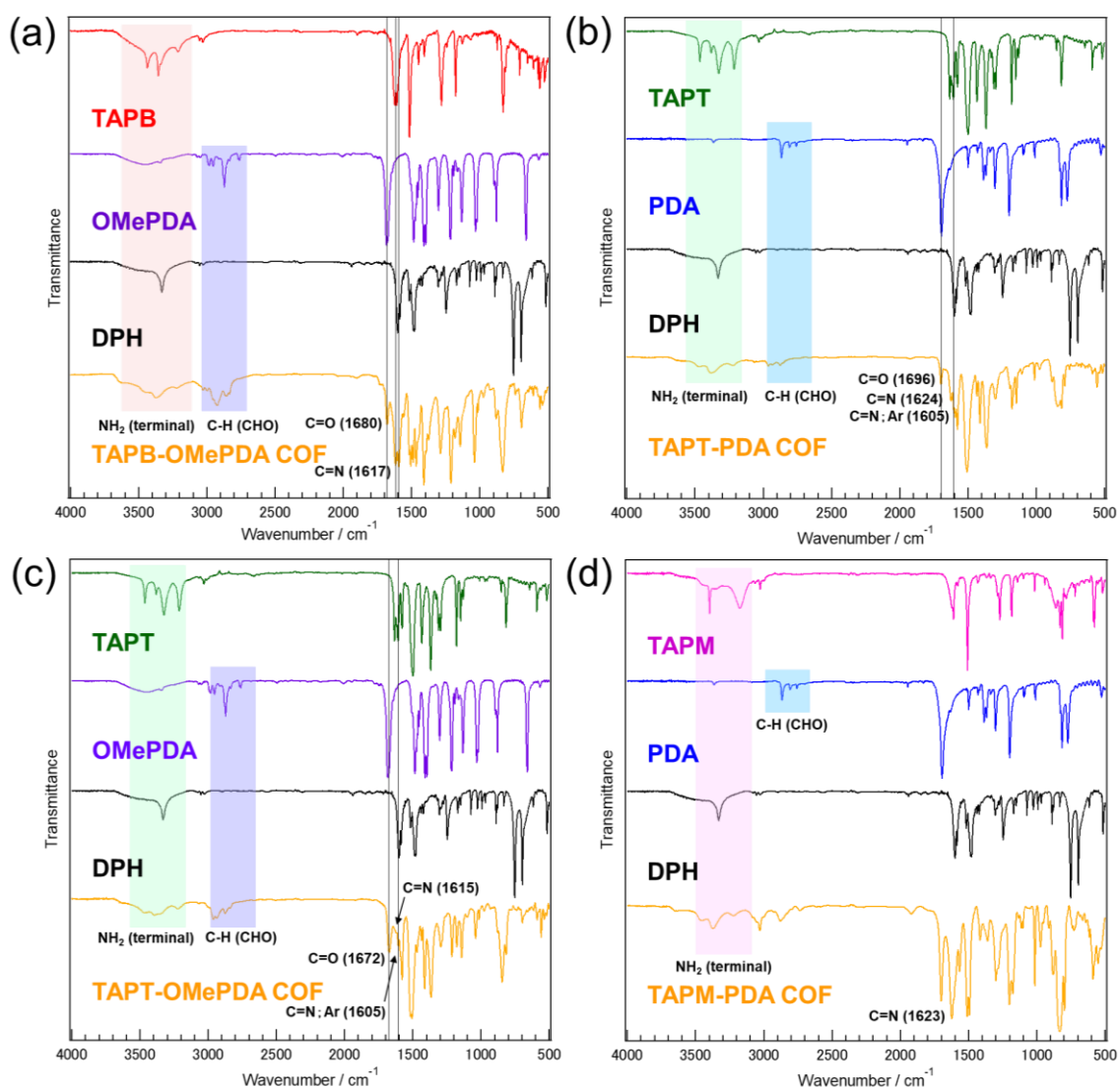


Figure S9. FT-IR spectra of COF and each component: (a) TAPB-OMePDA COF, (b) TAPT-PDA COF, (c) TAPT-OMePDA COF, (d) TAPM-PDA COF.

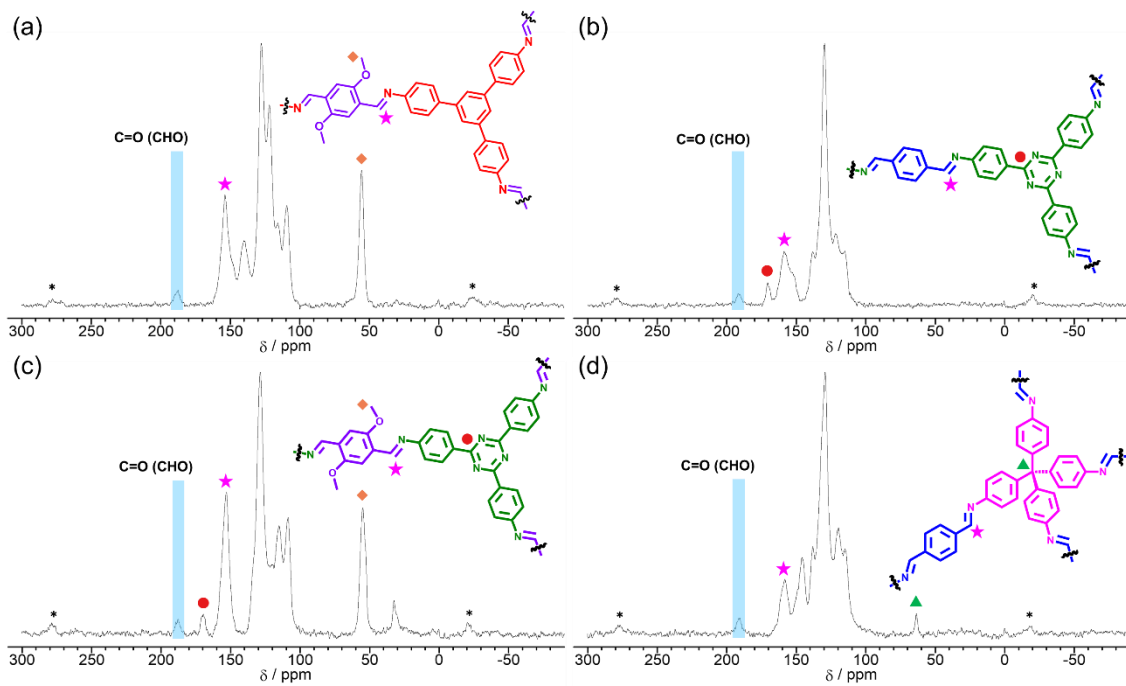


Figure S10. CP-MAS ^{13}C NMR spectra of (a) TAPB-OMePDA COF, (b) TAPT-PDA COF, (c) TAPT-OMePDA COF, (d) TAPM-PDA COF. Asterisks denote spinning sidebands.

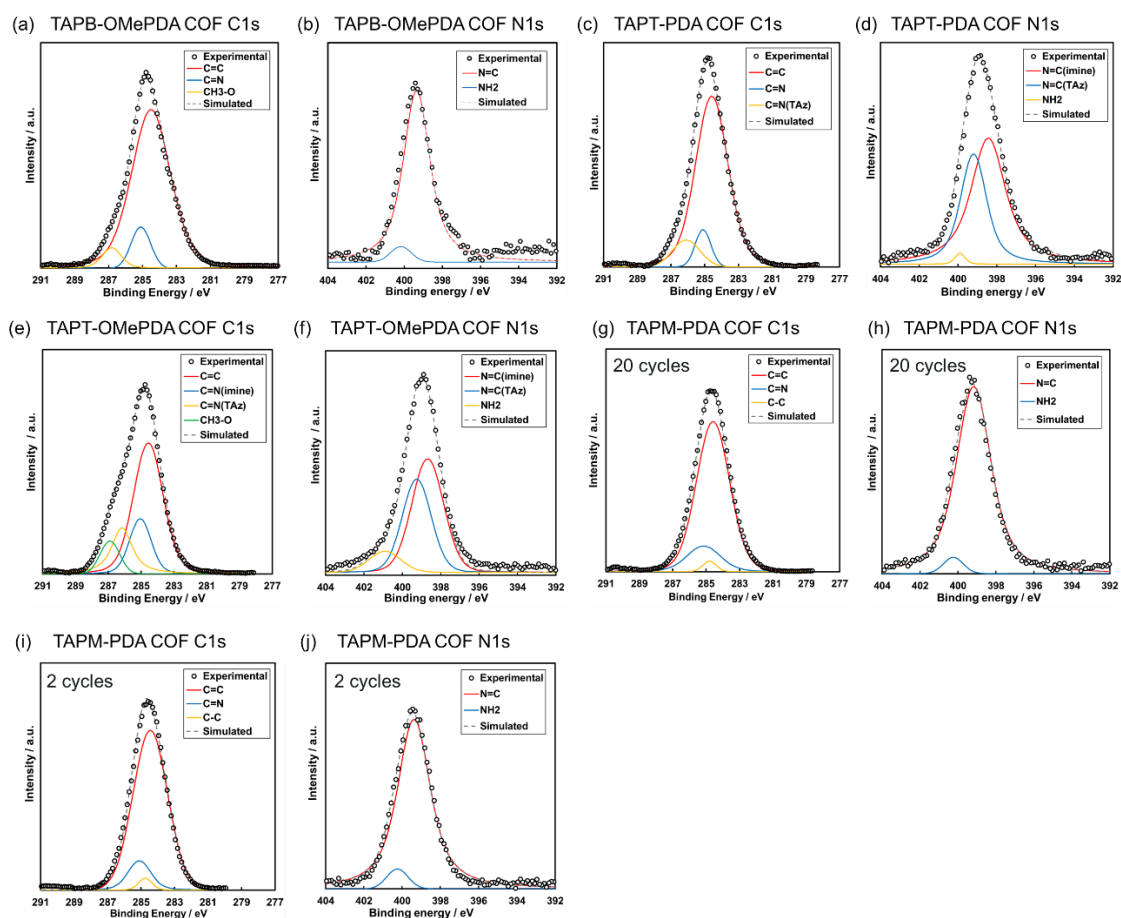


Figure S11. XPS spectra of (a,b) TAPB-OMePDA COF, (c,d) TAPT-PDA COF, (e,f) TAPT-OMePDA COF and (g-j) TAPM-PDA COF. (a,c,e,g,i) for C1s and (b,d,f,h,j) for N 1s peak. (a–h) the COF samples synthesized through 20 cycles of CV and (i,j) the samples synthesized through 2 cycles. Based on the comparison of (g,h) and (i,j), the electronic state of carbon and nitrogen in TAPM-PDA samples were not changed between the early stage and the mature stage.

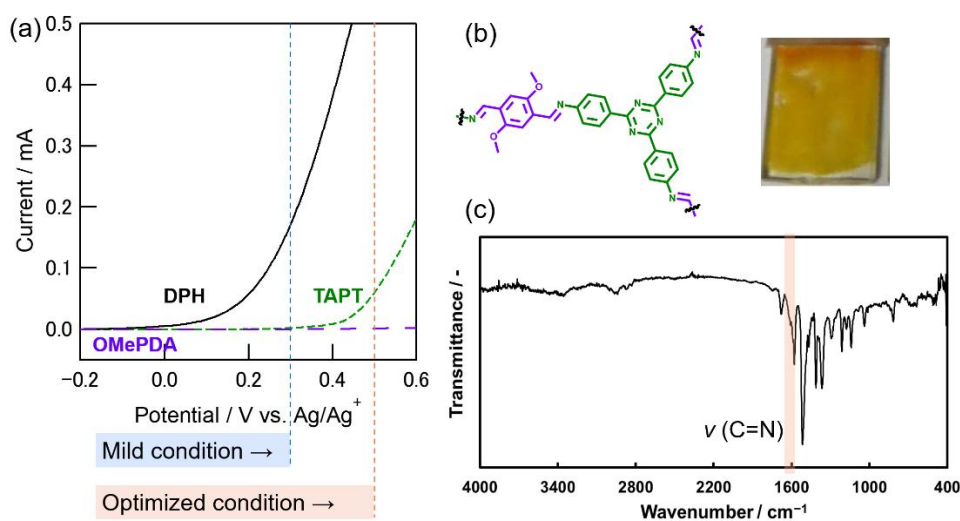


Figure S12. (a) Comparison between the optimized condition and the mild condition for COF synthesis. In the mild condition where the potential sweep range was between -0.5 and 0.3 V, the TAPT was not oxidized but the DPH was involved in the oxidation. (b) Photograph and (c) FT-IR spectra of TAPT-OMePDA COF synthesized through the potential range between -0.5 and 0.3 V vs. Ag/Ag⁺ (the mild condition).

The yellow TAPT-OMePDA film was also successfully obtained under the mild condition in which only DPH was oxidized. The EGA from DPH is a very essential factor for the COF formation.

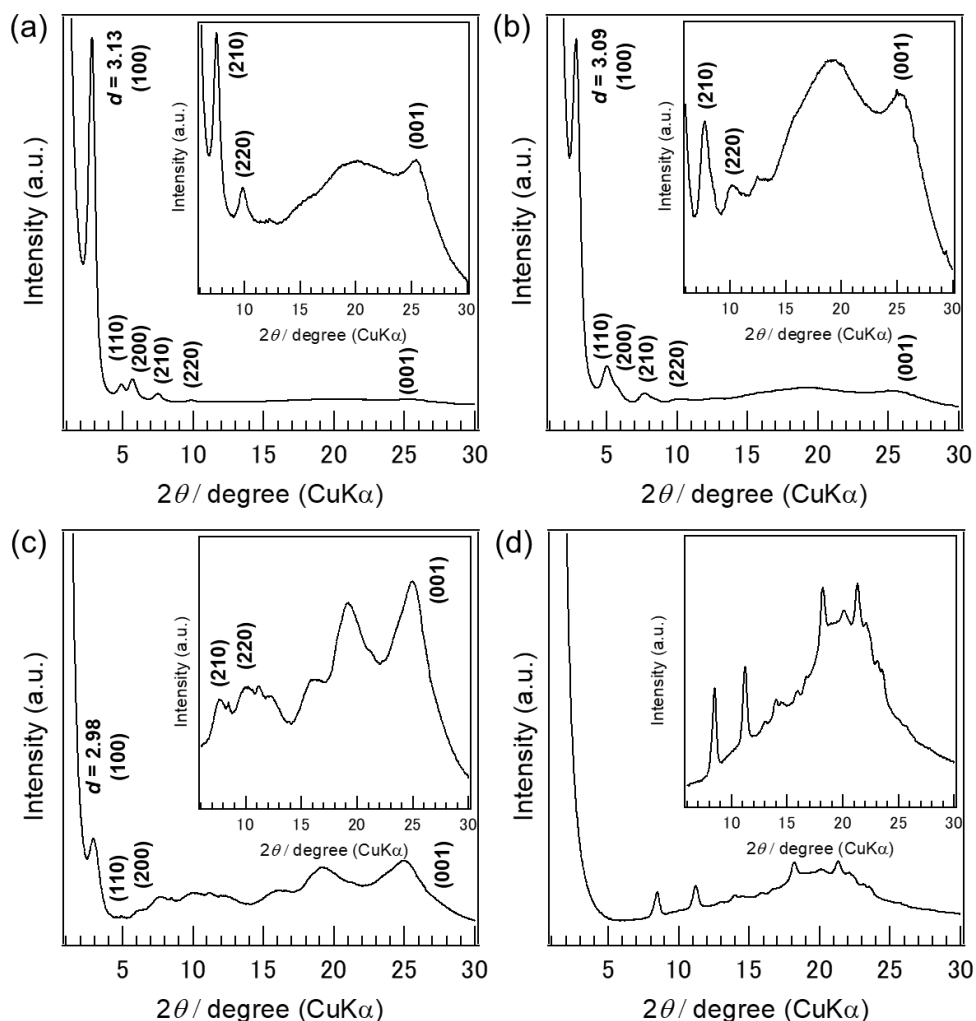


Figure S13. SAXS diffraction patterns of (a) TAPB-OMePDA COF, (b) TAPT-PDA COF, (c) TAPT-OMePDA COF, and (d) TAPM-PDA COF. The samples were rinsed with MeCN, MeOH and hexane, and activated by supercritical CO₂ drying.

(a) TAPB-OMePDA COF: the peak position of SAXS is $2\theta = 2.82^\circ, 4.92^\circ, 5.69^\circ, 7.50^\circ, 9.85^\circ, 25.40^\circ$ attributed to the (100), (110), (200), (210), (220), and (001) facets, respectively.

(b) TAPT-PDA COF: the peak position of SAXS is $2\theta = 2.86^\circ, 5.06^\circ, 5.72^\circ, 7.70^\circ, 10.12^\circ, 25.34^\circ$ attributed to the (100), (110), (200), (210), (220), and (001) facets, respectively.

(c) TAPT-OMePDA COF: the peak position of SAXS is $2\theta = 2.96^\circ, 4.94^\circ, 6.04^\circ, 7.70^\circ, 10.16^\circ, 25.10^\circ$ attributed to the (100), (110), (200), (210), (220), and (001) facets, respectively.

(d) TAPM-PDA COF: the peak position of SAXS is $2\theta = 8.49^\circ, 11.23^\circ, 18.20^\circ, 21.31^\circ$.

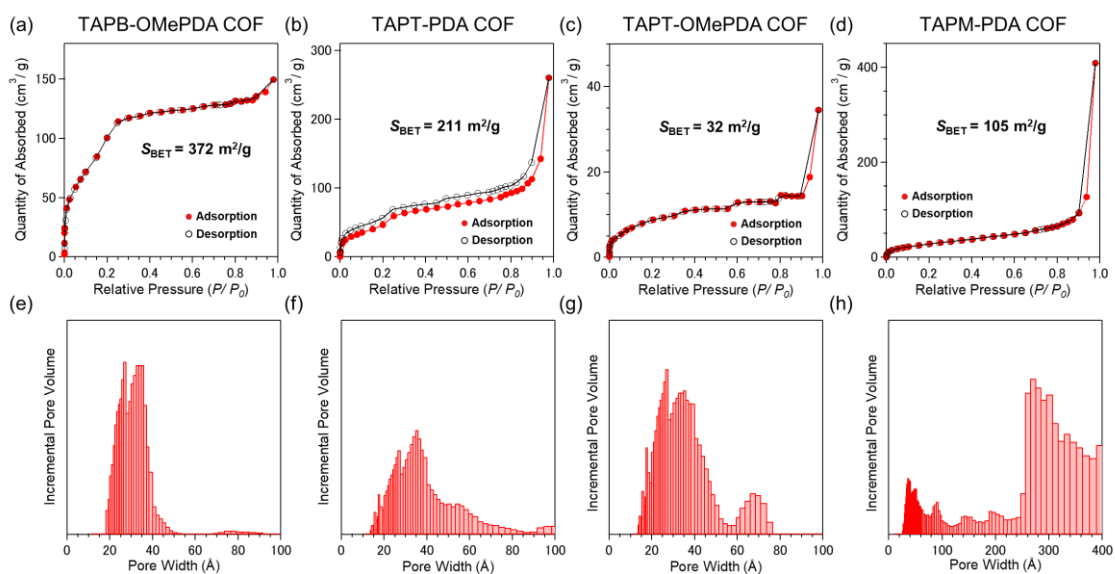


Figure S14. (a–d) N_2 adsorption (filled circles) and desorption (empty circles) isotherms (77 K). (e–h) NLDFT-calculated pore size distributions. The pore sizes and their distributions were determined using DFT models of cylinder carbon. These samples were rinsed with MeCN, MeOH and hexane, and activated by supercritical CO_2 drying.

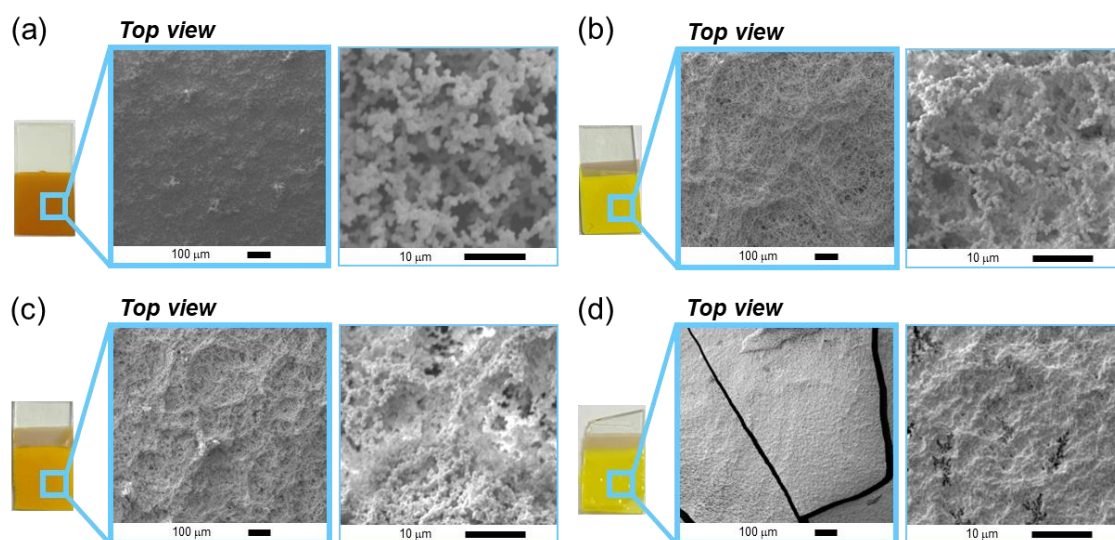


Figure S15. SEM images of (a) TAPB-OMePDA COF, (b) TAPT-PDA COF, (c) TAPT-OMePDA COF, and (d) TAPM-PDA COF films.

8. Reference

- (1) P.-W. Cheng, C.-Y. Chen, T. Ichibayashi, T.-F. M. Chang, M. Sone, S. Nishimura, *J. Supercrit. Fluids* **2022**, *180*, 105455.